HEAT TRANSFER CHARACTERISTICS OF PLATE EVAPORATOR USING ALUMINUM HERRINGBONE PLATE FOR OTEC

Hirofumi ARIMA [1]*, Yuta SHIGENAGA [2], Masanao NISHIGUCHI [2]

[1] Institute of Ocean Energy, Saga Univ., 1-48, Hirao, Kubara-aza, Yamashiro-cho, Imari-shi, Saga, 849-4256, Japan

[2] Graduate school of Sci. Eng., Saga Univ., 1-Honjo, Saga-shi, Saga 840-8502, Japan

*Corresponding Author: arima@ioes.saga-u.ac.jp

ABSTRACT

Ocean thermal energy conversion (OTEC) usually uses plate-type heat exchangers (PHEs) as an evaporator, condenser, and other devices. Generally, the heat transfer plate of PHEs is made of titanium because ammonia and seawater flow in PHEs as a working fluid and heat source. However, titanium is expensive and difficult to process; therefore, the use of low-cost materials is essential. The selection of materials for the heat transfer plates of a PHE is also a key factor affecting the OTEC performance. The suitability of aluminum alloy, Cu-Ni alloy, and stainless steel as materials for OTEC heat exchangers has been explored in some studies. The focus is on aluminum among other materials, because aluminum has better thermal conductivity than titanium, and its cost is also lower than that of titanium. The authors considered aluminum as an alternative to titanium. However, aluminum has low corrosion resistance for ammonia and seawater. To improve corrosion resistance, several coating methods are employed for aluminum, such as Polyether Ether Ketone (PEEK) resin or WIN KOTE® film, anodic oxidation, anodized and coated composite film; long-term immersion tests are conducted on ammonia. Anodic oxidation is identified as the best coating method to improve the corrosion resistance to ammonia. Therefore, anodic oxidation is employed in the aluminum coating method. Heat exchange and boiling experiments are performed on the apparatus used with ammonia to elucidate the thermal performance of aluminum alloy treated by anodic oxidation (1050 alloy) plate on the PHEs. In addition, the heat transfer performance is compared with three types of heat transfer surface shapes. As a result of the measurement of the overall heat transfer coefficient, the best configuration in these three plates is identified, and the overall heat transfer is almost the same as that of the titanium plate. In addition, the heat transfer coefficients of ammonia on these three plates are determined, and the value depends on the mass flow rate of ammonia. It is found that the anodized aluminum plate can be used as an evaporator, through which the ammonia flowed as a working fluid.

1 INTRODUCTION

Ocean thermal energy conversion (OTEC) systems generate electricity between the temperature difference of the surface (25-30 °C) and deep ocean water (5-10 °C) using ocean thermal energy. This system is constructed based on the Rankine cycle, and it has heat exchangers, such as an evaporator and condenser. OTEC system usually used “Plate heat exchangers (PHEs)”. As the heat exchanger has larger heat transfer area per volume, PHEs are used as heat exchangers, which saved space. In addition, OTEC usually used ammonia as the working fluid (Bharatha, 2011). The heat transfer performance of the evaporator and condenser significantly contributes to the efficiency of electricity generation of the entire cycle in the OTEC. In the design of a heat exchanger, it is important to clarify the date of the heat transfer coefficient. In a conventional study, the measurement of the heat transfer coefficient of ammonia on a plate heat exchanger was investigated by Kushibe *et al.* (2005, 2006), Kim *et al.* (2007), Okamoto *et al.* (2009), Djordjevic *et al.* (2008), and Sterner *et al.* (2006). Kim *et al.* (2007) and Okamoto *et al.* (2009) systematically measured the heat transfer coefficient of ammonia. On the other

hand, the improvement in the heat transfer performance of the evaporator is also important for improving the OTEC performance. Okamoto *et al.* (2009) clarified that the minute irregularities in the processing of the heat transfer surface promoted the nucleate boiling of ammonia, and the value increased by 20% - 40% against a flat surface. Koyama *et al*. (2014a, 2014b) confirmed that the heat transfer coefficient of the PHE improved by narrowing the channel gap size. Both investigations focused on heat transfer performance by improving the structure of the PHEs. However, there have been no studies on the materials used in the heat exchanger to improve the heat transfer performance. Kapranos *et al*. (1987) studied the material selection for OTEC design using stainless steel, titanium, Cu-Ni alloy, and aluminum. They concluded that the best material is titanium, because OTEC uses ammonia and seawater. On the other hand, the authors focused on aluminum, which has a higher thermal conductivity than titanium. However, aluminum has low corrosion resistance for ammonia and seawater; therefore, it is not suitable for use in OTEC without some processing. Following this, the authors devised coating heat transfer plates that were added to improve the corrosion resistance of PEEK resin and Diamond-Like Carbon (DLC), and they measured the heat transfer performance and ammonia corrosion resistance using the plates (Arima et al., 2018). It was found that these coating plates could be used in ammonia environments for approximately three months. However, the resin has a high cost of coating and high thermal resistance. The author investigated the corrosion resistance of aluminum using different material coating methods (Arima et al., 2020). It was clarified that anodized aluminum plate had the highest ammonia corrosion resistance and lowest thermal resistance. In addition, the cost of coating was lower than that of previous resin or DLC coatings. On the other hand, anodized aluminum plate has also high seawater resistance was clarified by Hagihara (1969). He performed the seawater immersion test during a year using different treated methods and compared the corrosion. As a result of the test, the immersed the anodized aluminum was observed the discoloration by attachment of marine life, however, the base material surface was not observed corrosion after surface cleaning. Incidentally, the author investigated the thermal performance of PHEs with aluminum flat plates. However, the practical use of PHEs involved the usage of herringbone-type plates, and there have been no studies on PHEs using aluminum herringbone plates. In this study, a new herringbone-type aluminum plate with anodic oxidation treatment is produced to evaluate ammonia's boiling heat transfer performance. In this paper, the results of the measurement of the overall heat transfer coefficient of PHE and the boiling heat transfer coefficient of ammonia are reported.

2 EXPERIMENT

2.1 Experimental apparatus

In this study, two types of tests are performed: hot-cold water (water – water) heat exchange and ammonia-forced convective boiling experiments. The experimental apparatus of the former is shown in Figure 1(a), and the latter is shown in Figure 1(b). Figure 1(a) consists of a test section (PHE), hot water tank, hot water pump, and refrigerator for heat sink. Figure 1(b) consists of a test section (plate evaporator), condenser, working fluid tank, sub-cooler, two refrigerators for heat sink, a hot water tank, a working fluid pump, and a hot water pump. Figure 1(b) also consists of a working fluid, hot water, and cold-water circuits. The test sections are plate-type heat exchangers (Alfa Laval: T2-BFG), condenser, and sub-coolers are brazed heat exchangers (Tokyo Braze: TB-MS11V); the working fluid pump is a magnet centrifugal pump (speck: NPY-2251MK0402, output: 500 W), the hot water pump is a magnet centrifugal pump (Sanso Electric: PMD-1523B6M, output 150 W), the heater in the hot water tank is an immersion heater (Hakko Electric: BWA3230, output 200 V–3 kW and BWA1120, output 100 V–2 kW), and two heat sinks are DC inverter chillers (Orion: RKW1500B-V-G1, cooling capacity: 5.3 kW and RKS753J-MV, cooling capacity: 2.5 kW).

The system quantities of the state are measured using several sensors. System temperatures are measured using K-type thermocouples (Hayashi Denko: ST6, class 1, accuracy ±1.5 °C). The system pressures are measured using a pressure transducer (Yokogawa: FP101, range: 0 – 2 MPa, accuracy: ± 0.25% F. S.). The mass flow rate of the working fluid is measured using a Coriolis mass flow meter (Endress+Hauser: PROMASS 83A, accuracy: within ± 0.1%). The flow rates of hot and cold water are measured using a magnetic volumetric flow meter (Keyence: FD-M50AT and FD-81 series, repeatability ± 1.6%FS.). This data is accumulated to a data logger (GRAPHTEC: GL-820).

2.2 Test section and test plate

The test section, which is a plate heat exchanger, consisted of two frames, i.e., a commercial product and four new aluminum plates that are produced in the present study. Figure 2 shows the design and appearance of the four types of test plates, and Table 1 lists the geometrical data of the test plate. Test plates are made of 1050 aluminum. The herringbone shape shown in Figure 2 is formed by press working. The plate has a height of 350 mm, width of 100 mm, thickness of 1 mm; the chevron angle on the plate surface is 45°, the pitch of the corrugate is 8.13 mm, and its height is 2.47 mm.

To make ammonia corrosion resistant, the plates are surface-treated by anodizing, as prescribed in JIS H8601. The thickness of the anodizing layer is approximately 20-25 μm. One set of four pieces of test plates is incorporated into the PHE. The specifications of the test plate with these test plates are listed in Table 2.

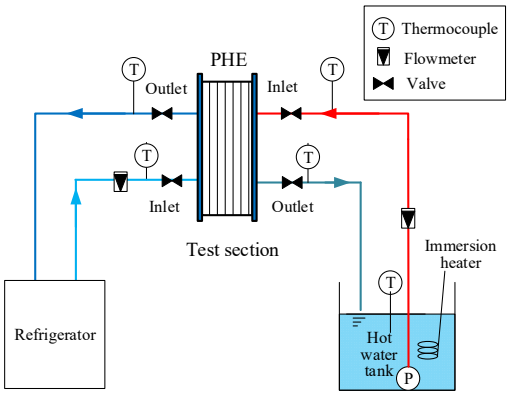

(a) Water-water heat exchange experiment.

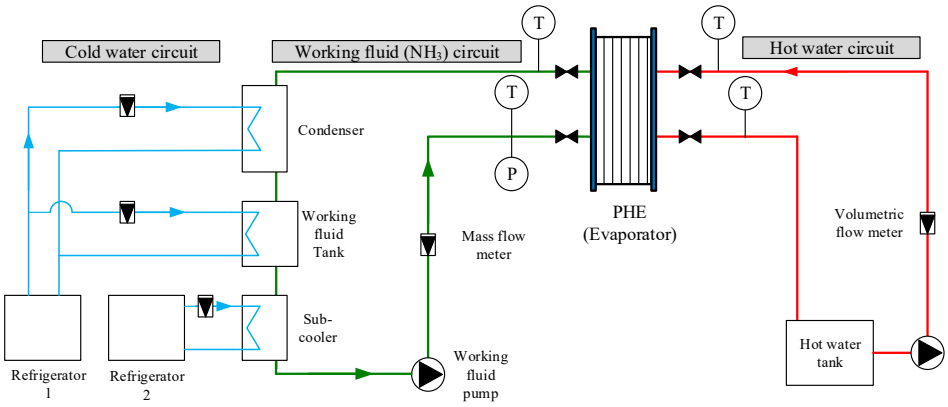

(b) Ammonia forced convective boiling experiment.

Figure 1: Schematic diagram of experimental apparatus.

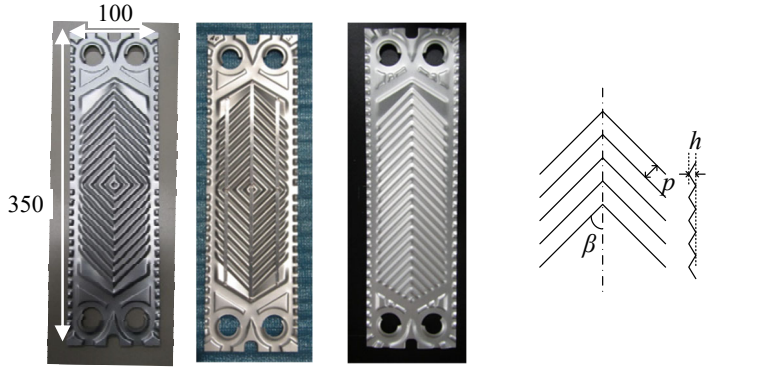

(a) TP-1 (b) TP-1R (c) TP-2 (d) Design of corrugate shape

Figure 2: Design of test plate.

Table 1 Geometrical data of the test plate.

Thickness	t	[mm]	1
Wave height	h	[mm]	2.47
Wave pitch	p	[mm]	8.13
Chevron angle	β	[deg]	45
Effective heat transfer area	A_s	[m^2/plate]	1.8 x 10^{-2}
Herringbone pattern	TP-1, TP-1R		Point symmetry
	TP-2		Line symmetry

Table 2: Specification of test section

Number of plates on test section	4
Number of channels (hot water/ working fluid sides)	3/2
Total heat transfer area A_s [m^2]	7.698×10^{-2}
Cross-sectional area of working fluid channel Ac_{wf} [m^2]	2.057×10^{-4}
Length of the heat transfer area of test plate l_{ch} [m]	0.239
Thermal conductivity of A1050 aluminum k [W/mK]	225

2.3 Experimental procedure

In this study, two different experiments using previously mentioned herringbone plates are performed: (1) measurement of the overall heat transfer coefficient in water-water exchange experiments, (2) measurement of the overall heat transfer coefficient and boiling heat transfer coefficient on ammonia forced convection boiling experiment and heat transfer performance is evaluated.

2.3.1 Heat exchange experiments on water-water: The apparatus used in the water-water heat exchange experiment is shown in Figure 1(a). The hot and cold water flowed into each side port of the test section and heat exchange is performed. In addition, both the water port temperature and flow rate are measured and accumulated on a data logger. The experimental conditions are presented in Table 3(a).

2.3.2 Experiment of forced convective boiling on ammonia: The ammonia boiling experiment is performed using the apparatus shown in Figure 1(b). The ammonia that is stored in the working fluid tank flowed into the test section through a working fluid pump, via a sub-cooler. The device cools ammonia with cold water from heat sink #2, and has the role of sustaining a supercooling state. The hot water at a predetermined temperature from the hot water tank is provided to the test section, and ammonia evaporated. two-phase or superheated ammonia flowed into the condenser from the test section and is condensed by the cold water from heat sink #1. The sub-cooled ammonia returned to the working fluid tank. In the present experiment, the temperature of the hot water inlet, ammonia outlet pressure, and flow rate of hot water and ammonia kept these values constant and maintained a steady state. All quantities of state are measured by several sensors, and the data logger is accumulated. The experimental conditions are presented in Table 3(b). Table 4 shows the number of runs on each test plate, TP-1, TP-1R, and TP-2.

2.4 Data reduction

2.4.1 Define the heat transfer coefficient of hot water: Water-water heat exchange experiments are performed to define the heat transfer coefficient of the hot water side of the test section. The value is derived as follows:

The heat transfer rate $\dot{Q}_h$ [W] is calculated using the following equation,

$$\dot{Q}_h = \dot{m}_h c_{ph}(T_{h,in} - T_{h,out}) \quad (1)$$

where $\dot{m}_h$ [kg/s] is the mass flow rate of hot water in the test section, c_{ph} [J/kgK] is the specific heat of hot water, and $T_{h,in}$ and $T_{h,out}$ [°C] are the temperatures of the inlet and outlet of the hot water side, respectively. c_{ph} and other properties of water are calculated using PROPATH (Propath Group, 2016). The overall heat transfer U_{ww} [W/m^2K] of the cold-hot water experiment is defined as follows:

Table 3: Experimental conditions

(a) Water-water heat exchange experiment

Hot water flow rate [L/min] ([m/s])	1, 2, 3, 4, 5, 6, 7 (0.081, 0.162, 0.243, 0.324, 0.406, 0.487, 0.567)
Cold water flow rate [L/min] ([m/s])	1 (0.081)
Hot water inlet temperature [ºC]	30, 40
Cold water inlet temperature [ºC]	5, 10

(b) Ammonia-forced convective boiling experiment

Hot water flow rate $\dot{m}_h$ [L/min] ([m/s])	1, 2, 3, 4, 5 ,6 (0.081, 0.162, 0.243, 0.324, 0.406, 0.487)
Working fluid mass flow rate $\dot{m}_{wf}$ [kg/h]	3.5, 5, 7.5, 10, 15
(Mass flux [kg/m^{2}s])	(7.1, 10.1, 15.2, 2.03, 3.04)
Hot water inlet temperature $T_{h,\,in}$ [ºC]	30, 40
Working fluid outlet pressure P [kPa_abs]	700

Table 4: Number of Runs on ammonia-forced convective boiling experiment

TP-1	87
TP-1R	98
TP-2	108

$$U_{ww} = \dot{Q}_h/(A_s\,\Delta T_{lm,ww}) \tag{2}$$

where A_s [m^2] and $\Delta T_{lm,ww}$ [°C] are the surface area of the test plates and the logarithmic mean temperature difference, respectively.
$\Delta T_{lm,ww}$ [°C] is defined as follows:

$$\Delta T_{lm,ww} = \frac{(T_{h,in}-T_{c,out})-(T_{h,out}-T_{c,in})}{\ln\frac{(T_{h,in}-T_{c,out})}{(T_{h,out}-T_{c,in})}} \tag{3}$$

where $T_{c,in}$ and $T_{c,out}$ [°C] are the temperatures of the inlet and outlet of the cold water side, respectively. The heat transfer coefficient, h_h, of the hot water side is calculated using Eq. (4), with the overall heat transfer coefficient U_{ww}, thermal conductivity k [W/mK] of the plate, and thickness t [m] of the plate.

$$1/U_{ww} = 1/h_h + 1/h_c + t/k \tag{4}$$

2.4.2 Define the heat transfer coefficient of ammonia: The overall heat transfer coefficient and boiling heat transfer of ammonia are derived as follows: Initially, the overall heat transfer coefficient U_{wf} (W/m^{2}K) is calculated using the following equation:

$$U_{wf} = \dot{Q}_h/(A_s\,\Delta T_{lm,wf}) \tag{5}$$

where $\dot{Q}_h$ [W], A_s [m^2], and $\Delta T_{lm,wf}$ [°C] are the heat transfer rate, surface area of the test plates, and logarithmic mean temperature difference, respectively. $\dot{Q}_h$ [W], $\Delta T_{lm,wf}$ [°C] are defined as follows:

$$\dot{Q}_h = \dot{m}_h c_{ph}(T_{h,in} - T_{h,out}) \tag{6}$$

$$\Delta T_{lm,wf} = \left(T_{h,in} - T_{h,out}\right)/\ln\frac{(T_{h,in}-T_{sat})}{(T_{h,in}-T_{sat})} \tag{7}$$

where m_h [kg/s] is the mass flow rate of hot water in the test section, c_{ph} [J/kgK] is the specific heat of hot water, and $T_{h,in}$ and $T_{h,out}$ [°C] are the temperatures of the inlet and outlet of the hot water side, respectively. T_{sat} [°C] is the saturated temperature, which is calculated using PROPATH (Propath Group, 2016). c_{ph} are also calculated using PROPATH.
On the other hand, the heat transfer coefficient h_{wf} of the ammonia side is calculated using Eq. (8) with the overall heat transfer coefficient U_{wf}, thermal conductivity k [W/mK] of the plate, and thickness t [m] of the plate.

$$1/h_{wf} = 1/U_{wf} - (1/h_h + t/k) \tag{8}$$

where, h_h derives from Nu correlations as discussed below.
Finally, the vapor quality x of the outlet of the ammonia side for the data reduction of boiling heat transfer is defined as follows:

$$x = \frac{\dot{Q}_h - \dot{Q}_{sub} - \dot{Q}_{sup}}{\dot{m}_{wf} L} \tag{9}$$

where L [J/kg] is the latent heat, and the mass flow rate of the working fluid is $\dot{m}_{wf}$ [kg/s]. $\dot{Q}_{sub}$ and $\dot{Q}_{sup}$ are the heat transfer rates of the sub-cool and superheated regions in the heat transfer area, respectively.
The uncertainties of the overall heat transfer coefficient and heat transfer coefficient of working fluid are about 3.5% and 25.5%, which are estimated by Moffat (1988) method. The uncertainties of the other data are subscribed in Table 5.

Table 5: Uncertainties of the measured and calculated parameters.

Parameter	Uncertainty
Pressure, P	± 0.25% F.S.
Temperature, T	± 0.1 ℃
Hot water volumetric mass flow rate, $\dot{m}_h$	± 1.6 %
Working fluid mass flow rate, $\dot{m}_{wf}$	± 0.1 %
Heat Transfer rate, $\dot{Q}_h$	± 2.7 %
Overall heat transfer coefficient, U	± 3.5 %
Heat transfer coefficient of working fluid, h_{wf}	± 25.5 %

3 RESULT

3.1 Measurement of heat transfer coefficient of hot water (Case: TP-1)

Figure 3 shows that the relationship between hot water velocity v_h and overall heat transfer coefficient U_{ww} of water-water using TP-1 test plates. In this experiment, the overall heat transfer coefficient is measured on varied hot water flow rate keeping cold water flow rate at 1 L/min. It is found that the overall heat transfer coefficient U_{ww} increased with an increase in hot water velocity v_h. In addition, the value increased by involution for hot water velocity. Therefore, the correlation between the heat transfer coefficient of the hot water side and the hot water velocity is derived using the Wilson plot method. First, n = 0.3 is obtained as a value of the involution from correlation between $1/v_h$ and $1/U_{ww}$. Next, $1/U_{ww}$ value is plotted against $1/v_h^n$ as shown in Figure 4 and constant of proportionality $C_{h1} = 5.52\times10^{-4}$ is obtained. Finally, the correlation of heat transfer coefficient of hot water is derived as follows;

$$h_h = 1.81 \times 10^3 {V_h}^{0.3} \tag{10}$$

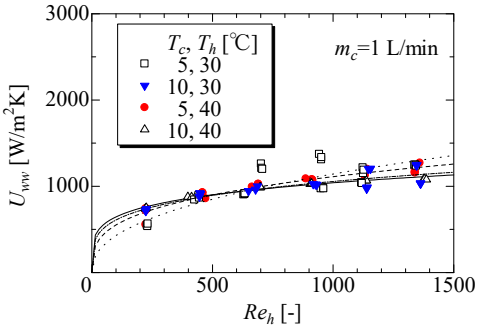

Figure 3: Overall heat transfer coefficient against *Re* number of hot water at TP-1 plate.

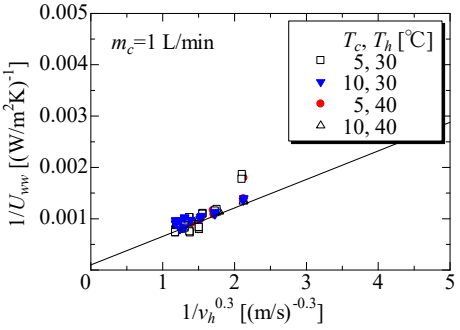

Figure 4: $1/U_{ww}$ vs. $1/v_h^{0.3}$ at TP-1 plate.

The hot water heat transfer coefficients of the TP-1R and TP-2 test plates are also derived using the same method. Subsequently, the Nusselt number correlations for each plate are derived using the previous hot water heat transfer coefficient as follows:

$$\text{TP-1:}\quad Nu = 0.300Re^{0.297}Pr^{1/3} \tag{11}$$

$$\text{TP-1R:}\quad Nu = 0.757Re^{0.292}Pr^{1/3} \tag{12}$$

$$\text{TP-2:}\quad Nu = 0.295Re^{0.637}Pr^{1/3} \tag{13}$$

Figure 5 shows that comparison of Nu number correlation between three different test plates. TP-2 plate yielded the best heat transfer coefficient among the three test plates.

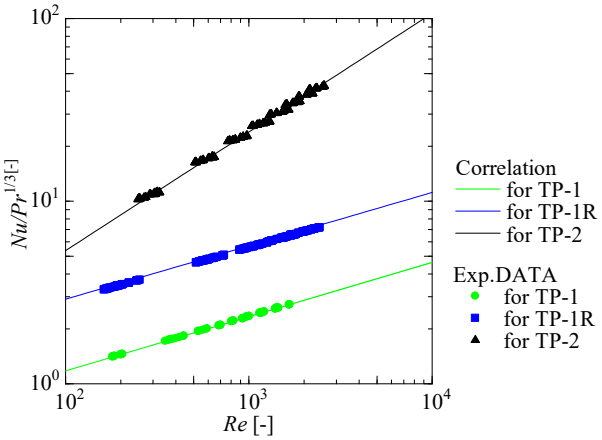

Figure 5: Relationship between Re and $NuPr^{-1/3}$

3.2 Measurement of overall heat transfer coefficient of evaporator

Figure 6 (a)–(c) show the relationship between the Re_h number of hot water and the overall heat transfer coefficient U_{wf} of the ammonia evaporator using three types of test plates. When comparing the overall heat transfer coefficients at different test plates, TP-2 yielded the best value at the maximum mass flow rate of the working fluid, which is m_{wf}= 15 kg/h. The value of TP-2 is approximately four times larger than TP-1, which is approximately 1.5 higher than TP-1R. In Figure 6 (a), the overall heat transfer increases with an increase in the *Re* number at each working fluid flow rate condition. There is no difference in the overall heat transfer based on the working fluid flow rate. In Figure 6 (b) and (c), the overall heat transfer decreases with an increase in the middle *Re* number at low working fluid flow rate conditions. This meant that the outlet working fluid conditions has high vapor qualities or superheat. Under these vapor conditions, the ammonia boiling heat transfer is lower than at lower vapor qualities. Subsequently, the overall heat transfer coefficient is also reduced.

By the comparison of the value of overall heat transfer in the same Re, the value of TP-2 plate shows the largest. This reason considerably depends on the difference equivalent diameter. The equivalent diameter of TP-2 (D_h = 4.94 mm) is about 2.5 times of TP-1 and TP-1R (D_h = 2 mm). Because the gap size of TP-1 is about half of TP-2, the pressure losses increase, and the water side velocity decreases. Thus, the heat transfer coefficient of the water side becomes small. The heat transfer of water side of TP-1 is small, the overall heat transfer coefficient of TR-1 also shows a small value. The pressure loss of TP-1R which is installed the spacer decreases, the heat transfer coefficient of water side is two times of TP-1 value. However, the overall heat transfer of TP-1R is as approximately same as that of TP-1. On the other hand, heat transfer coefficient of water side of TP-2 is larger than that of TP-1 and TP-1R, due to the gap size of TP-2 is about 2.5 times of those. Therefore, heat transfer coefficient of working fluid side of TP-2 increases, in conclusion, the overall heat transfer coefficient also increases.

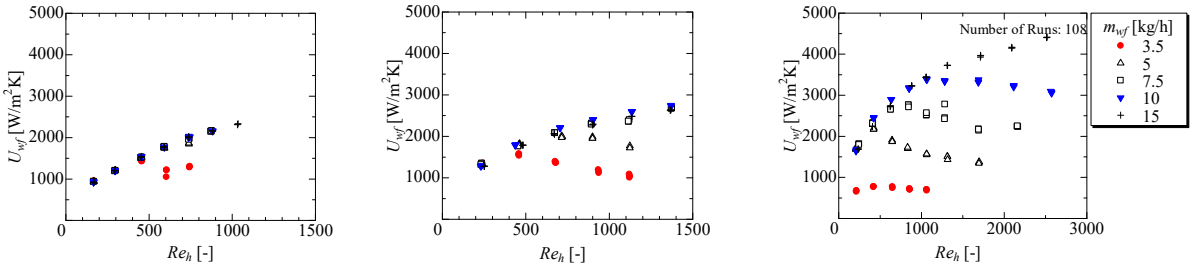

(a) TP-1 (b) TP-1R (c) TP-2

Figure 6: Overall heat transfer coefficient vs. hot water flow velocity.

4 CONCLUSION

The author produced a new herringbone-type aluminum test plate and evaluated its performance by measuring the overall heat transfer coefficient of the heat exchanger and the boiling heat transfer of ammonia.

(1) At the all-test plates, the influence of the working fluid flow rate on the overall heat transfer is not observed except of high vapor quality condition at the outlet of working fluid. As the overall heat transfer shows an approximately constant value at a high flow rate of hot water, it is observed that the heat transfer coefficient of water is governing.

(2) The overall heat transfer of TP-1 is the smallest in all test plates. The heat transfer coefficient of both sides is small, due to the gap size is half of TP-2.

ACKNOWLEDGEMENT

The authors wish to thank the Japan Keirin Association Foundation (JKA Foundation: 2019M-145) for providing research funds.

NOMENCLATURE

A_s,	Overall heat transfer are	(m^2)
c_p	Specific heat	(J/kgK)
h	Heat transfer coefficient	(W/m^2K)
L	Latent heat	(J/kg)
m	Mass flow rate	(kg/s)
P	Pressure	(Pa)
Q	Heat transfer rate	(W)
T	Temperature	(°C)
ΔT	Temperature difference	(°C)
t	Thickness of plate	(m)
U	Overall heat transfer coefficient	(W/m^2K)

v	Flow velocity	(m/s)

Greek

ρ	density	(kg/m^3)

Subscript

h	hot water
in	inlet
l	liquid phase
lm	legalistic mean
out	outlet
sat	saturated
wf	working fluid
ww	water-water experiment

REFERENCES

Wilson, E. E., 1915, A Basic for Rational Design of Heat Transfer Apparatus, *Transactions of ASME*, vol. 37: p. 47-70.

Hagihara, M., 1969, Studies on corrosion of surface-treated aluminum alloys in sea water, *Journal of Japan Institute of Light Metals*, vol. 19, no. 4: pp. 136-141.

Kapranos, P., Priestner, R., 1987, Overview of Metallic Materials for Heat Exchangers for Ocean Thermal Energy Conversion Systems, *Journal of Materials Science*, vol. 22: p. 1141-1149.

Moffat, R.J., 1988, Describing the uncertainties in experimental results, Experimental Thermal Fluid Science, vol. 1: p. 3-17.

Kushibe, M., Ikegami, Y., Monde, M., Uehara, H., 2005, Evaporation Heat Transfer of Ammonia and Pressure Drop of Warm Water for Plate Type Evaporator, *Trans. JSRAE*, vol. 22, no. 4: p. 403-415.

Kushibe, M., Ikegami, Y., Monde, M., Uehara, H., 2006, Evaporation Heat Transfer of Ammonia /Water Mixtures for Plate Type Evaporator, *Trans. JSRAE*, vol. 23, no. 4: p. 389-397.

Sterner, D., Sunden, B., 2006, Performance of plate heat exchangers for evaporation of ammonia, *Heat Transfer Engineering*, vol. 27, no. 5: p. 45-55.

Kim, J-H., Arima, H., Ikegami, Y., 2007, Fundamental Study of Local Heat Transfer in Forced Convective Boiling of Ammonia on Vertical Flat Plate, *Trans. JSRAE*, vol. 24, no. 3: p. 217-226.

Djordjevic, E., Kabelac, S., 2008, Flow Boiling of R134a And Ammonia in a Plate Heat Exchanger, *Int. J. Heat and Mass Trans.*, vol. 51: p. 6235-6242.

Okamoto, A., Arima, H., Kim, J-H., Akiyama, H., Ikegami, Y., 2009, Characteristic of Local Boiling Heat Transfer of Ammonia / Water Binary Mixture on the Plate Type Evaporator, *Trans. JSRAE*, vol. 26, no. 2: p. 131-139.

Bharathan, D., 2011, Staging Rankine Cycles Using Ammonia for OTEC Power Production, Technical Report NREL, TP-5500-49121.

Koyama, K., Chiyoda, H., Arima, H., Ikegami, Y., 2014a, Experimental Study on Thermal Characteristics of Ammonia Flow Boiling in a Plate Evaporator at Low Mass Flux, *Int. J. Refri.*, vol. 38: p. 227-235.

Koyama, K., Chiyoda, H., Arima, H., Okamoto, A., Ikegami, Y., 2014b, Measurement and Prediction of Heat Transfer Coefficient on Ammonia Flow Boiling in a Microfin Plate Evaporator, *Int. J. Refri.*, vol. 44: p. 36-48.

Propath Group, 2016, W-PROPATH, http://propath.mech.nagasaki-u.ac.jp/PROPATH/p-propath.html.

Arima, H., Matsuda, S., Inadomi, R., Suga, Y., Yamamoto, K., 2018, Heat Transfer Characteristic of a Heat Exchanger using Aluminum Alloy Plate for OTEC, *Proc. 6th Int. OTEC Sympo.*: G11.

Arima H., 2020, Ammonia corrosion resistance of surface-treated aluminum materials, *J. The Japan Institute of Light Metals*, vol. 70, no.5: p. 1-8.